OPEN ACCESS
IOP Publishing
Journal of Physics D: Applied Physics
J. Phys. D: Appl. Phys. **50** (2017) 065104 (9pp)
doi:10.1088/1361-6463/aa5006

Deep-level spectroscopy in metal–insulator–semiconductor structures

A Kurtz[1], E Muñoz[1], J M Chauveau[2] and A Hierro[1]

[1] ISOM and Dpto. Ingeniería Electrónica, Universidad Politécnica de Madrid, Ciudad Universitaria, 28040 Madrid, Spain
[2] Université Cote d'Azur, CNRS, CRHEA, 06560 Valbonne Sophia Antipolis, France

E-mail: adrian.hierro@upm.es

Received 28 September 2016, revised 21 November 2016
Accepted for publication 28 November 2016
Published 12 January 2017

Abstract

In this study we present a method for measuring bulk traps using deep-level spectroscopy techniques in metal–insulator–semiconductor (MIS) structures. We will focus on deep-level transient spectroscopy (DLTS), although this can be extended to deep-level optical spectroscopy (DLOS) and similar techniques. These methods require the modulation of a depletion region either from a Schottky junction or from a highly asymmetric p–n junction, junctions that may not be realizable in many current material systems. This is the case of wide-bandgap semiconductor families that present a doping asymmetry or have a high residual carrier concentration or surface carrier accumulation, such as InGaN or ZnO. By adding a thin insulating layer and forming an MIS structure this problem can be circumvented and DLTS/DLOS can be performed under certain conditions. A model for the measurement of bulk traps in MIS structures is thus presented, focusing on the similarities with standard DLTS, maintaining when possible links to existing knowledge on DLTS and related techniques. The model will be presented from an equivalent circuit point of view. The effect of the insulating layer on DLTS is evaluated by a combination of simulations and experiments, developing methods for the measurement of these type of devices. As a validation, highly doped ZnO:Ga MIS devices have been successfully characterized and compared with a reference undoped sample using the methods described in this work, obtaining the same intrinsic levels previously reported in the literature but in material doped as high as 1×10^{18} cm^{-3}.

Keywords: spectroscopy, metal–insulator–semiconductor, deep levels, defects, characterization, simulation

(Some figures may appear in colour only in the online journal)

1. Introduction

Deep-level spectroscopy techniques are powerful tools for assessing the presence of electrically active defects in semiconductor materials [1, 2]. Among them, deep-level transient spectroscopy (DLTS) [1] has been one of the most widely used techniques, where the presence of deep levels is quantified through the analysis of the transient change of junction capacitance due to thermal emission of the trapped carriers. Its principle of operation was extended later to deep-level optical spectroscopy (DLOS) [2], where the emission of carriers from the traps is obtained by optical excitation, but where the physical processes involved are generally the same. While with DLTS only the bandgap region below ~1 eV from the conduction band can be probed in n-type material, with DLOS the rest of the bandgap down to the minority carrier band can be analyzed. This is especially useful for the case of heavily compensated material, where one wishes to quantify the incorporation

of acceptors in n-type material (or donors in p-type material) [3–7]. However, both DLTS and DLOS rely on the use of specific devices in which a depletion region is well defined, such as in highly asymmetric p–n junctions (where the depletion region drops on the lightly doped side of the junction) or Schottky junctions. Still, both of these devices pose great technological difficulties for many materials of current interest. First, some materials suffer from large surface carrier accumulation or conductivity, in which Schottky contacts are not feasible. This is the case for InGaN alloys, which show high surface carrier accumulation [8] and which, similarly to ZnO [9] and CdO [10], impede the formation of Schottky contacts. Moreover, many wide-bandgap materials present difficulties with one of the doping types, so-called doping asymmetry [11], hindering the realization of p–n junctions. Finally, and even if p–n junctions could be realized in a given material system, the need to have an asymmetric p–n junction with at least an order of magnitude difference in the doping level between both sides (to ensure that the depletion region drops mostly on the lightly doped side) may be unreachable in material systems where the residual carrier concentration is high.

MIS structures are a suitable solution for circumventing these limitations since they avoid most of the aforementioned difficulties. Therefore, by extending the knowledge of DLTS/DLOS for bulk deep-level analysis to MIS devices in a controlled way, and by properly quantifying the new effects this insulating layer generates on the techniques, a wider range of materials could be analyzed. Moreover, not only could DLTS/DLOS be performed on MIS structures, but other techniques based on modulating the depletion region will be affected in a similar way and benefit from such understanding. A good example of the role that an MIS structure has is ZnO, where the surface is passivated to allow the formation of a rectifying Schottky junction [12–15]. In this material, the surface is typically treated with H_2O_2 [13, 14, 16], which induces the formation of a thin insulating layer [14]. However, even if the current–voltage (*I*–*V*) curves resemble those of a Schottky diode, there could be a hidden MIS structure that can strongly affect the capacitance transient behavior of the device, as it has already been observed in ZnMgO:N measured by DLOS [7].

Early results using MIS devices for DLTS analysis mainly focused on probing interface states, pulsing the device into accumulation or inversion. Just a few years after Lang first described the basis of DLTS [1], several studies were published that applied the technique to insulator-based devices [18–23]. The first report by Wang *et al* [17] used IGFETs to measure only interface traps, with a theoretical discussion on the procedure, which was further improved by Schulz *et al* [18], and Özder *et al* [19, 20] in Si MOS structures. The most thorough report on the measurement of bulk states instead of surface states, in MOS diodes, was published by Yamasaki *et al* [21]. In their work, the processes of carrier emission from bulk states were analyzed, obtaining very similar expressions to those from DLTS. However, they failed to point out the similarities between the measurement processes for MIS and Schottky/p–n diodes, despite the presence of an insulating layer. Also, their model did not consider the transient effects coming from the presence of the insulator, i.e. they assumed the voltages to be constant, which is not a complete description, as will be shown in this paper. Several years later, Nakashima *et al* [22] extended that work, adding an investigation of MOS on SOI structures, describing the measurement for lock-in DLTS, but again lacking a complete study of the voltage and timing regimes in MIS devices and the proper design of the experiments. Our work further expands and simplifies the analysis of DLTS in MIS devices, comparing the obtained spectra with those measured in a non-insulator-affected sample, which is of great importance in materials with native insulating layers that are difficult to characterize and for the measurement of semiconductors with a high carrier concentration (intrinsic or from doping), in which the design of the experiment is crucial to maximize the sensitivity of the measurement.

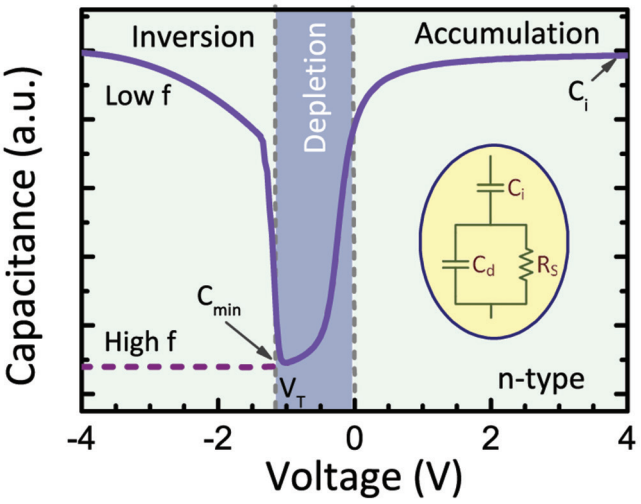

Figure 1. Metal–insulator–semiconductor capacitance–voltage profile for n-type material indicating the different operating regimes. Inset: equivalent circuit for an MIS structure in the depletion regime.

2. Theoretical model

2.1. Basic MIS theory

As thoroughly explained in textbooks [23], MIS devices show different operating modes (accumulation, depletion and inversion) as a function of semiconductor doping levels, insulator characteristics and applied bias. Depending on the operating mode, the region of the material being probed using spectroscopic techniques varies largely, and has to be taken into account when analyzing the experimental data.

Recalling the equivalent electrical circuit for an MIS structure (inset of figure 1), it can be observed that the total capacitance will be the series combination of two capacitances, the insulator capacitance (C_i) and the semiconductor depletion region capacitance (C_d)

$$C_{\text{total}}(t) = \frac{C_d(t) \cdot C_i}{C_d(t) + C_i}. \quad (1)$$

The semiconductor resistance has also been included in the equivalent circuit, since the insulator charge and discharge

processes will occur mainly through that resistance under normal circumstances, i.e. in the absence of high leakage in the insulating layer.

The MIS structure has a capacitance–voltage (C–V) profile that indicates the aforementioned operating regimes (figure 1). It can be observed that under inversion there is a difference between the high- and low-frequency curves, due to the time constant involved in minority carrier diffusion towards the surface needed for the formation of the inversion layer. However, for the purpose of material spectroscopy techniques, we will focus on the depletion regime, since it is the one that exposes the bulk material beneath the structure so that the existing deep levels can be filled and emptied, modulating the depletion volume. Under this regime, it is important to mention that there is no significant impact of the probe frequency associated with the insulating layer, despite the effect in the limit frequency posed by the presence of deep levels for capacitance measurements [24]. Therefore, standard capacitance/impedance meters can be used (normally working at 1 MHz in order to improve the signal-to-noise ratio).

Two parameters are indicated in figure 1 which are important for understanding MIS structures operating in the depletion regime. The first one, $C_{\min}$, is reached when the width of the depletion region is maximum ($W_{\mathrm{d,max}}$), just before the inversion layer is formed and no more depth modulation can be achieved [23]. It poses an effective limit on the depth that can be measured during the spectroscopy scans, and is indicated by the expression

$$C_{\min} \propto W_{\mathrm{d,max}}^{-1} \approx \sqrt{\frac{4\epsilon kT \ln\left(\frac{N_{\mathrm{D}}}{n_{\mathrm{i}}}\right)}{q^2}}, \tag{2}$$

where N_D denotes the carrier concentration in the film.

The second important parameter is the threshold voltage (V_{T}) [23], which assuming an ideal MIS structure with no trapped oxide charge and no differences in the metal/oxide/semiconductor work functions is given by

$$V_{\mathrm{T}} = \frac{kT}{q} \ln \frac{N_{\mathrm{D}}}{n_{\mathrm{i}}} - \sqrt{\frac{4\epsilon kTN_{\mathrm{D}} \ln\left(\frac{N_{\mathrm{D}}}{n_{\mathrm{i}}}\right)}{C_{\mathrm{i}}}}. \tag{3}$$

Both expressions show similar dependences on carrier concentration, temperature and the insulator capacitance. Moreover, and as it will be explained in the following section, the capacitance arising from the depletion region depends both on carrier concentration and applied voltage, both being parameters ($C_{\min}$ and V_{T}) modified during time as a result of carrier capture and emission processes, which are the basis for capacitance spectroscopy techniques.

2.2. MIS structures for deep-level spectroscopy

In this section we present our model for the steady state and transient operation in MIS devices for capacitance spectroscopy techniques, which are based on fill pulses (optical, electrical or both). The analysis of the relative effects introduced by the insulating and semiconductor layers will be analyzed.

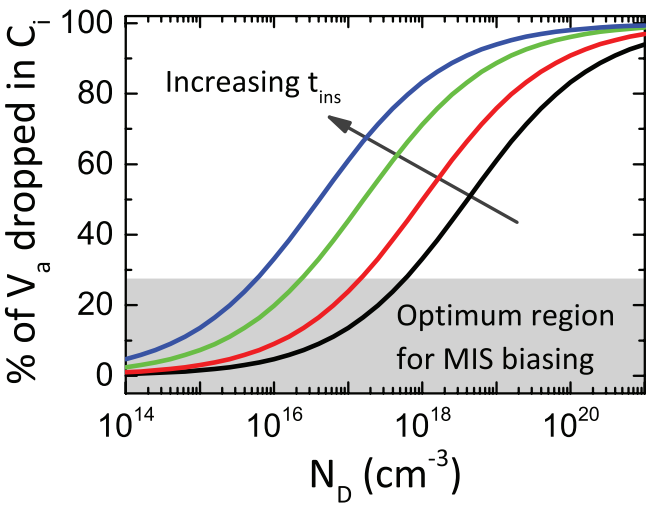

Figure 2. Percentage of the applied voltage dropping in the insulator as a function of doping concentration and insulator thickness ($t_{\mathrm{ins}} = 10, 20, 50, 100$ nm). The graph is compiled assuming a static dielectric constant of 8.7 (ZnO).

2.2.1. Steady state operation. Under steady state operation, the applied voltage (V_{a}) on an MIS structure will have to drop between the insulating layer (V_{i}) and the depletion in the semiconductor film (V_{d}) as

$$V_{\mathrm{d}} + V_{\mathrm{i}} = V_{\mathrm{a}}. \tag{4}$$

Since the charge in the insulator and the semiconductor are the same,

$$V_x = \frac{Q_s}{C_x};\ \text{Where } x = \begin{cases} \mathrm{i}: \text{ insulator} \\ \mathrm{d}: \text{ depletion} \end{cases} \tag{5}$$

and accounting for equation (1), then

$$V_{\mathrm{i}} = V_{\mathrm{a}} \frac{C_{\mathrm{d}}}{C_{\mathrm{d}} + C_{\mathrm{i}}}. \tag{6}$$

Therefore, the smaller the capacitance of the insulator (the thicker the layer), the larger the voltage drop in it. Figure 2 shows the relative amount of the applied voltage (V_{a}) that will drop in the insulator layer as a function of its thickness for various carrier concentrations in a given sample. This graph has been generated for a material with a static dielectric constant of 8.7 (ZnO), although for materials with different dielectric constants there will only be a horizontal shift in the curves. Ideally, it is desirable that the sample is designed to operate in the lower part of the graph, in order to maximize the control over the depletion voltage by minimizing the voltage drop in the insulator. This will be generally the case for very thin insulating layers, such as those created unintentionally by means of surface treatments or oxidation processes, considering the usual range of values for dielectric constants in semiconductors and native insulators. Moreover, by proper control of the voltage drop in the depletion region (V_{d}), depth-sensitive measurements could be carried out.

It is also important to mention that for thin insulators, and as a consequence of figure 2, samples with carrier concentrations as high as 10^{18} cm^{-3} could be measured provided that a satisfactory model is developed. As indicated above, such a

high doping regime is typically inaccessible for DLTS/DLOS because of the difficulty processing Schottky diodes or heavily doped asymmetric p–n junctions.

2.2.2. Transient effects in MIS structures. It can be recalled that during DLTS scans [1] samples are subjected to repeated bias square pulses. Under transient operation following the DLTS/DLOS fill pulse, time variation in bias has to be considered and modeled accordingly. The first and most obvious transient behavior following the electrical fill pulse will be the rearrangement of electric fields inside the structure. As previously indicated, the applied voltage has to drop between the insulator and the semiconductor. However, this process is not immediate and it affects the transient operation of the structure. Since for deep-level spectroscopy it is assumed that in the depletion region ($\Delta C_d/C_{d,\infty} \ll 1$) the depletion width changes relatively little compared to the overall background width, the charge or discharge process due to the insulating layer can be assumed to be nearly independent of the changes in depletion charge due to deep-level emission or capture processes.

If we now recall figure 1 and apply general circuit theory, the transient voltage drop in the insulator can be written as

$$V_i(t) = V_{i,\infty} \cdot (1 - e^{-t \cdot e_i}), \tag{7}$$

where $e_i^{-1} = R_s \cdot C_i$ and R_s can be obtained from the I–V characteristics of the device, whereas $V_{i,\infty}$ can be calculated from equation (6). The time constant for this expression has been written in terms of emission rate, in order to make it comparable to the term coming from the emission from deep levels (usually denoted by e_n or e_p depending on the carrier involved in the process). However, the MIS structure does not fully behave as its equivalent circuit may suggest, since a change in the voltage applied to the semiconductor induces a change in the depletion capacitance that further affects the overall shape of the measured capacitance transient, which will no longer have a simple exponential behavior as in a regular junction device.

The charge in the semiconductor, which affects the total measured capacitance, depends not only on the applied bias but also on the total carrier concentration in the depletion region and on the emission and capture processes following a change in the applied bias, as shown by

$$C_d(n,t) = A\sqrt{\frac{q\epsilon[N_D + n(t)]}{2[V_{bi} + V_d(t)]}}, \tag{8}$$

where

$$n(t) = N_T \times e^{-e_n \cdot t} \tag{9}$$

is the time-dependent carrier concentration due to emptying the deep levels after the voltage fill pulse.

We can observe in equation (8) that the capacitance in the depletion region is affected both by the changes in voltage coming from fill pulses $\{V_d(t)\}$ and by the change in carrier concentration in the semiconductor $\{n(t)\}$. This latter processes are the basis for the deep-level spectroscopy techniques, and imply the existence of thermal or optical excitation of the trapped carriers.

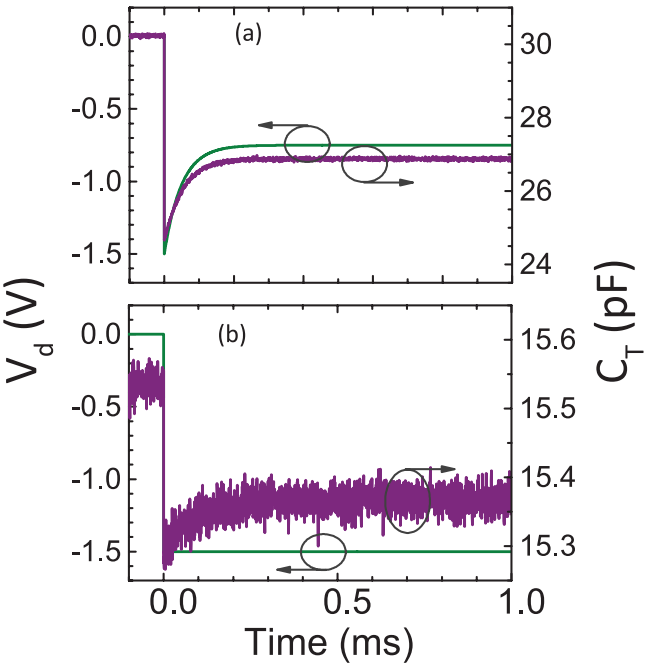

Figure 3. Simulated transients from the voltage drop at the depletion region (V_d) and total MIS capacitance (C_T) for (a) the insulator-dominated and (b) the depletion-dominated regimes after applying an external fill pulse from 0 to −1.5 V. White Gaussian noise has been added computationally.

Since the total capacitance that will be measured by the experimental system on an MIS structure is the series combination of the insulator capacitance and depletion capacitance (figure 1), we have to combine equations (1) and (7)–(9), yielding a general expression for the transient capacitance measured in an MIS diode right after a voltage fill pulse

$$C_{total}(t) = \frac{C_i}{1 + C_i\sqrt{\dfrac{V_{bi} + V_a\left[1 - \frac{C_{d,\infty}}{C_{d,\infty}+C_i}(1 - e^{-t \cdot e_i})\right]}{0.5q\epsilon(N_D + N_T e^{-t \cdot e_n})}}}. \tag{10}$$

In this equation, depending on the relative relationship between the exponential terms, two regimes can be distinguished:

- Insulator-dominated regime ($e_n \gg e_i$), where the emission from deep levels is faster than the change in voltage, so its small-amplitude transient will be undetectable from the overall transient, masked by the larger change due to the voltage effects.
- Depletion-dominated regime ($e_n \ll e_i$). If the emission from deep levels is much slower than the emission from the insulator, the voltage will be able to stabilize fast enough for the measurement system to be sensitive to the emission from deep levels, which is smaller in magnitude.

2.3. Simulation of DLTS spectra on MIS structures

The two regimes discussed in the previous section, insulator- or depletion-dominated, will have different effects on the total MIS capacitance and on the voltage drop in the depletion region (figure 3).

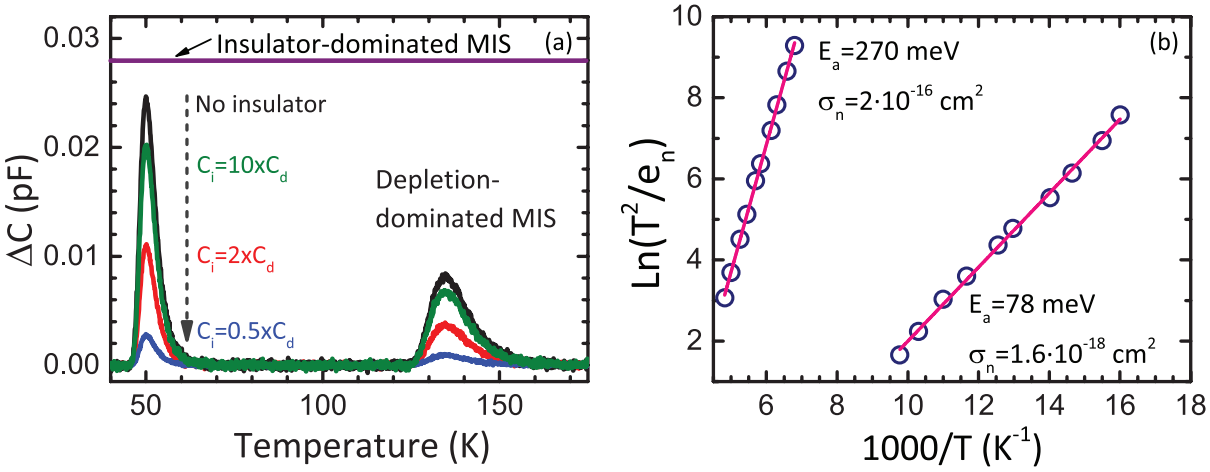

Figure 4. (a) Effect of the insulator layer under the insulator-dominated regime and reduction in peak height in the depletion-dominated regime for various C_i/C_d combinations. Spectra obtained from transients with added white Gaussian noise. (b) Arrhenius plot extracted for the two traps in (a). The DLTS spectra assumes two traps present at $E_C - 78$ meV and $E_C - 270$ meV with capture cross sections of 2×10^{-18} cm^{-2} and 2×10^{-16} cm^{-2}, and trap concentrations of of 2×10^{14} cm^{-3} and 5×10^{14} cm^{-3}, respectively. A residual carrier concentration of 1×10^{16} cm^{-3} is assumed.

In the case of the insulator-dominated transient, we can observe that the capacitance follows the depletion voltage transient, which will be slightly temperature dependent. This effect will create a nearly flat DLTS spectrum, as shown in figure 4, with no information about the presence of defects inside the depletion layer.

In the depletion-dominated regime, as indicated in equation (10) and figure 4, the amplitude of the simulated change in capacitance is reduced from that which will come from a non-MIS sample. The height of the peaks will be lowered depending on the ratio between the insulator and depletion capacitances. In this regime, the emission from deep levels close to the edge of the depletion region can be analyzed using the theory found in the DLTS literature [1, 16, 24]. Although voltage and charge values are related, since the changes in the capacitance in the depletion region after emptying the traps are assumed to be small ($\Delta C_d/C_{d,\infty} \ll 1$), both the insulator and depletion region voltages can be presumed constant. Therefore, the previously analyzed charge process in the insulator capacitor can be neglected, leaving as the dominant processes the charge transients present in the depletion region following an external voltage pulse.

Because of the serial combination of capacitors, the total change in capacitance (ΔC_{total}) of the MIS structure after a fill pulse will in fact be lower than that of a structure without the insulating layer. Using the time-dependent capacitance from equation (10) under the depletion-dominated regime, a general expression for the amplitude of the transient, related to the amplitude of the depletion transient, can be found as

$$\begin{aligned}\Delta C_{total} &= C_{total}(t \to \infty) - C_{total}(t = 0) \\ &= \frac{C_i^2 \Delta C_d}{(C_i + C_{d,\infty})(C_i + C_{d,\infty} - \Delta C_d)},\end{aligned} \tag{11}$$

which can be rewritten as

$$\Delta C_{total} = \frac{C_i^2 \frac{\Delta C_d}{C_{d,\infty}}}{(C_i + C_{d,\infty})(\frac{C_i}{C_{d,\infty}} + 1 - \frac{\Delta C_d}{C_{d,\infty}})}. \tag{12}$$

Since $\Delta C_d/C_{d,\infty} \ll 1$, then equation (12) can be simplified to

$$\begin{aligned}\Delta C_d &\approx \alpha \cdot \Delta C_{total} \\ &= \Delta C_{total} \cdot \frac{C_{d,\infty}(C_i + C_{d,\infty})(\frac{C_i}{C_{d,\infty}} + 1)}{C_i^2},\end{aligned} \tag{13}$$

where α is a correctivity factor given by

$$\alpha = \frac{C_{d,\infty}(C_i + C_{d,\infty})(\frac{C_i}{C_{d,\infty}} + 1)}{C_i^2}. \tag{14}$$

Once ΔC_d has been determined from the measured ΔC_{total}, the trap concentration can be obtained from the regular expression used in DLTS/DLOS [1, 2, 24]

$$N_T = 2N_D \frac{\Delta C_d}{C_{d,\infty}}. \tag{15}$$

The correctivity factor (α) indicates the relative reduction in the DLTS magnitude compared with that of a non-MIS sample. If $\alpha \approx 1$, the measurement will nearly perfectly match the spectra coming only from the depletion layer, which is the regime in which ideally the samples should be designed to operate. If α is close to unity, the value for the insulator capacitance does not need to be precisely known in order to have an accurate measurement of the trap concentration. Indeed, the experimental evaluation of this parameter is complicated, since C_i depends on the thickness of the insulating layer, which is difficult to obtain. However, because of the asymptotic definition of α, a low value of C_i will be sufficient.

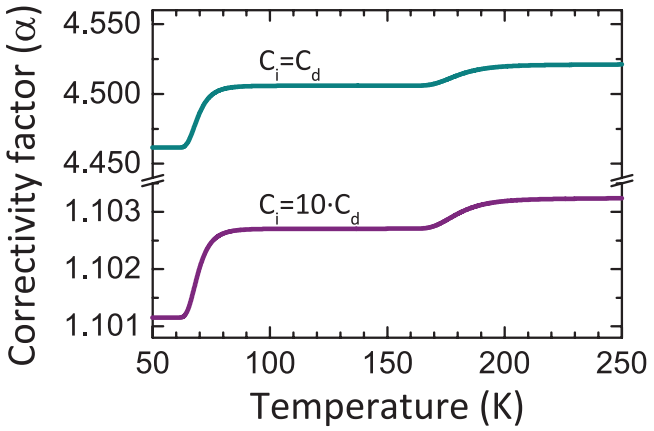

Figure 5. Correctivity factor for two cases where the insulator capacitance is similar and much larger than the depletion capacitance. Two traps are assumed at $E_C - 78$ meV and $E_C - 270$ meV with capture cross sections of 2×10^{-18} cm^{-2} and 2×10^{-16} cm^{-2} and trap concentrations of of 2×10^{14} cm^{-3} and 5×10^{14} cm^{-3}, respectively. A residual carrier concentration of 1×10^{16} cm^{-3} is assumed.

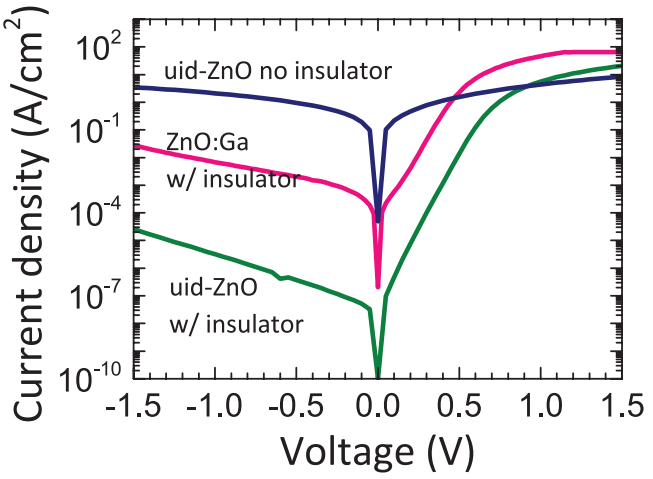

Figure 6. *I–V* curves without an insulator and with an insulating layer for the undoped ZnO and the highly doped ZnO:Ga samples (uid, unintentionally doped).

Besides, the limit on the doping level that can be obtained will be posed by the material becoming degenerate. This is especially valuable in the case of surface treatments in which the final thickness of the obtained insulating layer is quite thin.

When the insulator and depletion capacitance are similar, then $\alpha \approx 1$, and the trap concentration in an MIS diode can easily be derived by knowing the values of C_i and $C_{d,\infty}$. In the case of highly doped samples, or more generally those in which $C_i \approx C_d$, the measured change in capacitance will be lower than that arising purely from the emission from the deep level ($\alpha > 1$). Since the accurate evaluation of both C_i and $C_{d,\infty}$ is affected by a large experimental error, the trap concentrations obtained when $\alpha > 1$ will also show an increased uncertainty in their value. However, although exact calculation of the trap densities may not be feasible, a good approximation is made possible by knowledge of the relative magnitude of both capacitances. Simultaneously, the reduction in amplitude sets a limit to the effective sensitivity to trap concentrations. In this case, in order to reduce the effect of noise in the measurement, advanced correlation techniques, such as Fourier DLTS [25, 26], can be used to analyze the obtained transients.

The simulated DLTS spectra in figure 4 also show that independently of the variation of the peak height, the peak temperature positions are not modified. Therefore, the Arrhenius plot obtained in an MIS structure will be the same as that which would be measured in the absence of the insulating layer (figure 4(b)).

Figure 5 shows the temperature dependence of the correctivity factor for two different cases. In the sample where the insulator has a similar capacitance to the depletion layer, the measured DLTS spectra (and therefore the trap concentration) will be lower by a factor larger than four. On the other hand, if C_i is much larger than C_d, the trap concentration obtained from the DLTS measurement will be close to the real concentration of the trap obtained from equation (15).

Finally, an additional important effect that should be considered from the timing point of view is that during the fill pulse bias the capture rates are usually much faster than the emission rates for a given deep level. This makes the fill pulse behave as insulator-dominated, increasing the time needed to fully fill the traps by changing the depletion width. Therefore, as a general rule, the fill pulse should be set to be stable after at least three time constants of the insulator ($R_s \cdot C_i$) circuit. Moreover, for fill-pulse-dependent measurements (normally used to differentiate types of defects [27]), the correct analysis of the real applied pulse is complicated and will need an accurate knowledge of the capacitances and resistances at different temperatures, which are outside the scope of the present work. During the fill pulse it is also possible to drive the MIS device into accumulation, with the formation of a majority carrier layer on the surface. These effects will change the transient operation of the device after the fill pulse, and can be useful for the measurement of surface states, something that has been thoroughly described in the literature [17–20].

3. DLTS analysis on MIS test structures

Once the general expressions have been modeled and simulated for the transient effects in an MIS structure, this section will demonstrate the applicability of this model to MIS test devices measured by DLTS. In order to validate the simulations, two homoepitaxial MBE-grown m-ZnO samples were processed: an unintentionally (uid) doped ZnO sample and a highly doped ZnO:Ga sample. A standard H_2O_2 treatment [14, 16] was performed in both samples prior to the deposition of a Au layer, obtaining a thin insulating layer which is needed to achieve high rectification and that was shown to also create an MIS behavior [7, 14, 28]. As can be observed in figure 6, without the treatment, even for the undoped sample, no rectification is obtained because of the highly conductive layer that appears on the surface [15] which yields an Ohmic contact. In the samples processed after the treatment, rectification is obtained, which indicates modulation of the band bending, and thus the generation of a depletion region that can be used for DLTS measurements. *C–V* profiling yielded

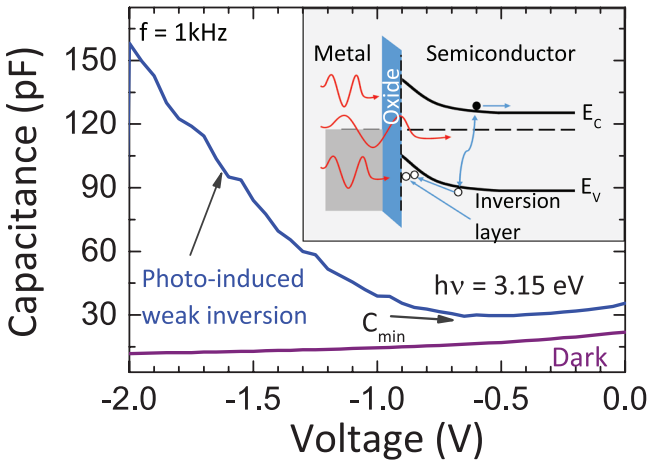

Figure 7. *C–V* profile under illumination for the undoped sample at 1 kHz. The inset shows the effect of the inversion layer.

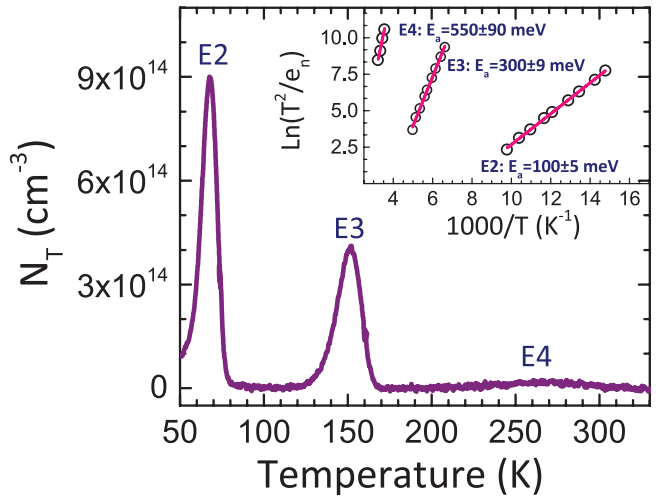

Figure 8. DLTS measurement (Rate Window $= 2\,s^{-1}$) for the undoped ZnO sample. $V_r = -1.5$ V, $V_{fill} = 0$ V, $t_{fill} = 50$ ms. The measurement was performed using the double boxcar analysis. Inset: Arrhenius plot showing the three obtained levels.

a carrier concentration of $\sim 1 \times 10^{16}$ cm^{-3} for the undoped sample, whereas the Ga-doped sample shows $\sim 1 \times 10^{18}$ cm^{-3}. Such high doping makes the realization of rectifying Schottky diodes extremely difficult, and thus DLTS in such highly doped samples is uncommon.

In order to validate the presence of the insulating layer, *C–V* profiles under illumination were performed at low frequencies (1 kHz), driving the sample into a weak inversion regime, as shown in figure 7. We can observe that due to the photogenerated carriers the shape of the *C–V* profile changes from a depletion shape towards a weak inversion profile from an MIS structure on n-type material. This effect has previously been described in detail in ZnMgO:N films [7]. From the work in [7, 13, 28] the insulating layer is known to be ~10 nm thick since identical H_2O_2 treatments were used on ZnO, which will yield an insulator capacitance of ~250 pF. This, combined with the total measured capacitances during the DLTS scans (~10 pF, see below), shows that the correctivity factor is $\alpha \approx 1$ for these samples.

DLTS was performed on these films with a 50 ms fill pulse at 0 V, and a reverse bias of −1.5 V. The time constant of the sample ($R_s \cdot C_i \approx 10$ ms) is much lower than the 50 ms fill pulse time (~5 time constants), and thus the traps can be assumed to be totally filled, without significant distortion from the insulating layer. Figure 8 shows the resulting spectrum and Arrhenius plot for the undoped sample, in which three intrinsic bulk traps E2, E3 and E4 are observed. Their trap characteristics, including energy, capture cross section and concentration, are summarized in table 1. The spectrum is dominated by the shallowest trap E2, at $E_C - 100$ meV, and with the highest concentration of all traps, $N_T = 9.3 \times 10^{14}$ cm^{-3}. Trap E3 is deeper, at $E_C - 300$ meV, and has a slightly lower concentration ($N_T = 4 \times 10^{14}$ cm^{-3}). Finally, the E4 level shows a trap concentration of $N_T = 2 \times 10^{13}$ cm^{-3}, over three orders of magnitude below the sample carrier concentration ($N_D = 1 \times 10^{16}$ cm^{-3}), a range which is typically taken as the trap detection limit in double boxcar DLTS. These intrinsic levels have been previously observed by other authors in ZnO grown by different methods [29–32], further emphasizing their intrinsic origin, and thus the validity of the measurement in a sample with an insulating layer on the surface that does not distort the obtained DLTS spectra. Furthermore, since the correctivity factor is close to unity, no significant reduction in the peak amplitude is produced, and the trap concentration can be directly derived from the DLTS spectrum in figure 8.

The highly doped ZnO:Ga sample could not be measured by the original double boxcar DLTS technique because of the low signal-to-noise ratio arising from the high doping level. Thus, Fourier DLTS (FDLTS) was used, which yielded spectra that were less affected by noise, as shown in figure 9. The previously dominant E2 level ($N_T = 9.3 \times 10^{14}$ cm^{-3} in the undoped sample) as well as E4 ($N_T = 2 \times 10^{13}$ cm^{-3} in the undoped sample) no longer appear in the highly doped sample, either because they are not present or they are below the detection limit. However, the FDLTS spectrum and Arrhenius plot confirm the presence of the previously observed E3 trap, with nearly the same energy, capture cross section and concentration ($N_T \approx 4 \times 10^{14}$ cm^{-3}), now over three orders of magnitude below the carrier concentration. Indeed, the comparison of the Arrhenius plot for E3 in both samples (inset of figure 9) indicates that it is the same trap, whose concentration is unaffected by the presence of Ga, which in combination with results from other authors ([29–32]), further reinforces its intrinsic origin.

Table 1 summarizes the results, and we can observe that the same intrinsic E3 bulk trap is present in both the undoped and highly doped ZnO samples, showing the same trap energy, concentration and capture cross section. Thus, as a result of the insulating layer induced by the H_2O_2 treatment, and despite the large doping level in the ZnO:Ga sample ($N_D \sim 1 \times 10^{18}$ cm^{-3}), DLTS could be performed on an MIS structure and the trap parameters were fully quantified following the theoretical model developed in section 2.

Table 1. Summary of the obtained deep levels for the ZnO MIS structures by DLTS. Units: activation energy (E_a): meV; trap concentration (N_T): cm^{-3}; capture cross section (σ_n): cm^2.

	ZnO undoped	ZnO:Ga
E2 ($E_a = 100$)	$N_T = 9.3 \times 10^{14}$ $\sigma_n = 5 \times 10^{-18}$	Not observed
E3 ($E_a = 300$)	$N_T = 3.7 \times 10^{14}$ $\sigma_n = 8 \times 10^{-16}$	$N_T = 4 \times 10^{14}$ $\sigma_n = 6 \times 10^{-16}$
E4 ($E_a = 550$)	$N_T = 2 \times 10^{13}$ $\sigma_n = 2 \times 10^{-16}$	Not observed

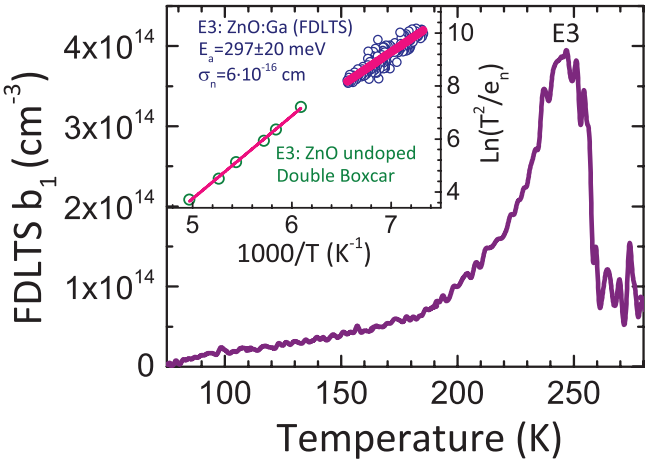

Figure 9. FDLTS spectra for the highly doped ZnO:Ga sample. $V_r = -1.5$ V, $V_{fill} = 0$ V, $t_{fill} = 50$ ms. Inset: Arrhenius plot showing the E3 level for both samples.

4. Conclusions

In this work we have developed and tested a theoretical model to allow the realization of deep-level spectroscopy techniques on MIS structures, addressing both the steady state behavior and transient operation after an electrical fill pulse. The dynamics of the device are highly dependent on the proportional relationship between the insulator and depletion capacitances, as summarized by the correctivity factor (α) shown in equation (14). This parameter offers a quick indication of the similarity of the obtained measurement with that from a sample in which a Schottky diode was processed without the insulating layer. If the insulator capacitance is large enough (much larger than the depletion capacitance), its exact value does not need to be precisely known in order to get accurate measurements of the trap concentrations. Also, the timing constraints that this layer induce have been analyzed, obtaining two different regimes under which the device can operate when pulsed electrically: insulator-dominated ($e_n \gg e_i$) and depletion-dominated ($e_n \ll e_i$). In the first one, the voltage transient coming from the charge and discharge processes in the insulator dominates the transient operation of the MIS device, masking the transient generated by the emission of carriers from the deep levels. Under the depletion-dominated regime, as has been simulated for DLTS, only a reduction in amplitude is obtained that can be neglected under the right conditions ($\alpha \approx 1$), but the time dependence of the traps is unmodified as is the Arrhenius plot and the parameters extracted from it: capture cross section and trap energy. Lastly, in order to maintain the operation of the device under the depletion mode, the MIS threshold voltage should be considered, especially if measuring at low frequencies, so the device does not shift to the inversion mode.

This theoretical model has been validated with MIS devices processed on two ZnO samples, an undoped one ($N_D \sim 1 \times 10^{16}$ cm^{-3}) and another one highly doped with Ga ($N_D \sim 1 \times 10^{18}$ cm^{-3}). By means of a low-frequency *C–V* profile under near-bandgap illumination, the presence of the insulating layer was assessed, and DLTS and FDLTS measurements were performed on both samples. Three intrinsic defects were obtained for the undoped sample, with one of them also being observable in the highly doped sample. This level, labeled E3 in the literature [29–31], shows the same trap energy, concentration and capture cross section in both samples, which is a clear indication of the validity of a DLTS measurement in an MIS device processed in a highly doped sample. The method of creating this insulating layer in order to allow the measurement of such materials has thus proven valuable and can be extended to other materials and/or dopants.

Acknowledgments

This work was funded by the Spanish Ministry of Economy and Competitiveness (MINECO) through project nos TEC2011-28076-C02-01 and TEC2014-60173-C2-2 and grant no. BES-2012-051882, and from the European Union's Horizon 2020 research and innovation program under grant agreement no. 665107 (project ZOTERAC). Growth at CRHEA-CNRS was partially supported by the French National Agency through the young researcher project ANR 11-JS09-014 HENOPOIN2.

References

[1] Lang D V 1974 Deep-level transient spectroscopy—new method to characterize traps in semiconductors *J. Appl. Phys.* **45** 3023–32

[2] Chantre A, Vincent G and Bois D 1981 Deep-level optical spectroscopy in GaAs *Phys. Rev.* B **23** 5335–59

[3] Armstrong A, Green D, Arehart A R, Mishra U K, Speck J S and Ringel S A 2005 Carbon-related deep states in compensated n-type, semi-insulating GaN:C, their influence on yellow luminescence *Symp. on GaN, AlN, InN and their Alloys held at the 2004 MRS Fall Meeting* (*Materials Research Society Symp. Proc.* vol 831) (Warrendale, PA: Materials Research Society) pp 311–6

[4] Armstrong A, Arehart A R and Ringel S A 2005 A method to determine deep level profiles in highly compensated, wide band gap semiconductors *J. Appl. Phys.* **97** 083529

[5] Gur E, Tabares G, Arehart A, Chauveau J M, Hierro A and Ringel S A 2012 Deep levels in a-plane, high Mg-content $Mg_xZn_{1-x}O$ epitaxial layers grown by molecular beam epitaxy *J. Appl. Phys.* **112** 123709

[6] Hierro A, Tabares G, Ulloa J M, Munoz E, Nakamura A, Hayashi T and Temmyo J 2009 Carrier compensation by deep levels in $Zn_{1-x}Mg_xO$/sapphire *Appl. Phys. Lett.* **94** 232101

[7] Kurtz A, Hierro A, Munoz E, Mohanta S K and Nakamura A 2014 Acceptor levels in ZnMgO:N probed by deep level optical spectroscopy *Appl. Phys. Lett.* **104** 081105

[8] Bailey L R, Veal T D, King P D C, McConville C F, Pereiro J, Grandal J, Sanchez-Garcia M A, Munoz E and Calleja E 2008 Band bending at the surfaces of In-rich InGaN alloys *J. Appl. Phys.* **104** 113716
[9] Brillson L J *et al* 2012 Interplay of native point defects with ZnO Schottky barriers and doping *J. Vac. Sci. Technol.* B **30** 050801
[10] Jefferson P H, Hatfield S A, Veal T D, King P D C, McConville C F, Zuniga-Perez J and Munoz-Sanjose V 2008 Bandgap and effective mass of epitaxial cadmium oxide *Appl. Phys. Lett.* **92** 022101
[11] Zunger A 2003 Practical doping principles *Appl. Phys. Lett.* **83** 57–9
[12] Brillson L J and Lu Y C 2011 ZnO Schottky barriers and Ohmic contacts *J. Appl. Phys.* **109** 121301
[13] Kashiwaba Y, Abe T, Nakagawa A, Niikura I, Daibo M, Fujiwara T and Osada H 2013 Formation of a ZnO_2 layer on the surface of single crystal ZnO substrates with oxygen atoms by hydrogen peroxide treatment *J. Appl. Phys.* **113** 113501
[14] Nakamura A and Temmyo J 2011 Schottky contact on ZnO nano-columnar film with H_2O_2 treatment *J. Appl. Phys.* **109** 093517
[15] Singh C S, Agarwal G, Rao G D, Chaudhary S and Singh R 2011 Effect of hydrogen peroxide treatment on the electrical characteristics of Au/ZnO epitaxial Schottky diode *Mater. Sci. Semicond. Process.* **14** 1–4
[16] Gu Q L, Ling C C, Chen X D, Cheng C K, Ng A M C, Beling C D, Fung S, Djurisic A B, Lu L W, Brauer G and Ong H C 2007 Hydrogen peroxide treatment induced rectifying behavior of Au/N–ZnO contact *Appl. Phys. Lett.* **90** 122101
[17] Wang K L and Evwaraye A O 1976 Determination of interface and bulk-trap states of IGFETs using deep-level transient spectroscopy *J. Appl. Phys.* **47** 4574–7
[18] Schulz M and Johnson N M 1977 Transient capacitance measurements of hole emission from interface states in MOS structures *Appl. Phys. Lett.* **31** 622–5
[19] Ozder S, Atilgan I and Katircioglu B 1996 Effects of surface potential fluctuations on DLTS of MOS structure *Solid State Electron.* **39** 243–9
[20] Ozder S, Atilgan I and Katircioglu B 1996 New approach to bias scan DLTS for rapid evaluation of interface states in MOS structures *Solid State Electron.* **39** 1507–14
[21] Yamasaki K, Yoshida M and Sugano T 1979 Deep level transient spectroscopy of bulk traps and interface states in Si MOS diodes *Japan. J. Appl. Phys.* **18** 113–22
[22] Nakashima H, Wang D, Noguchi T, Itani K, Wang J L and Zhao L W 2004 Method for detecting defects in silicon-on-insulator using capacitance transient spectroscopy *Japan. J. Appl. Phys.* **43** 2402–8
[23] Blood P and Orton J W 1992 *The Electrical Characterization of Semiconductors: Majority Carriers and Electron States* (*Techniques of Physics*) 1st edn (Oxford: Academic)
[24] Sze S M 2006 Semiconductor devices *Physics of Semiconductor Devices* (*Physics of Wiley*) 3rd edn (New York: Wiley)
[25] Ikeda K and Takaoka H 1982 Deep level Fourier spectroscopy for determination of deep level parameters *Japan. J. Appl. Phys.* **21** 462–6
[26] Weiss S and Kassing R 1988 Deep level transient Fourier spectroscopy (DLTFS)—a technique for the analysis of deep level properties *Solid State Electron.* **31** 1733–42
[27] Hierro A, Arehart A R, Heying B, Hansen M, Speck J S, Mishra U K, DenBaars S P and Ringel S A 2001 Capture kinetics of electron traps in MBE-grown N–GaN *Phys. Status Solidi* B **228** 309–13
[28] Nakamura A, Hayashi T, Hierro A, Tabares G, Ulloa J M, Munoz E and Temmyo J 2010 Schottky barrier contacts formed on polar and nonpolar $Mg_xZn_{1-x}O$ films grown by remote plasma enhanced MOCVD *Phys. Status Solidi* B **247** 1472–5
[29] Auret F D, Goodman S A, Legodi M J, Meyer W E and Look D C 2002 Electrical characterization of vapor-phase-grown single-crystal ZnO *Appl. Phys. Lett.* **80** 1340–2
[30] Auret F D, Nel J M, Hayes M, Wu L, Wesch W and Wendler E 2006 Electrical characterization of growth-induced defects in bulk-grown ZnO *Superlattices Microstruct.* **39** 17–23
[31] Auret F D *et al* 2007 Electronic properties of defects in pulsed-laser deposition grown ZnO with levels at 300 and 370 meV below the conduction band *Phys. B: Condens. Matter* **401** 378–81
[32] Muret P, Tainoff D, Morhain C and Chauveau J M 2012 Donor and acceptor levels in ZnO homoepitaxial thin films grown by molecular beam epitaxy and doped with plasma-activated nitrogen *Appl. Phys. Lett.* **101** 122104